

UETTrack: A Unified and Efficient Framework for Single Object Tracking

Ben Kang¹, Jie Zhao^{1,*}, Xin Chen², Wanting Geng¹, Bin Zhang¹, Lu Zhang¹, Dong Wang¹, Huchuan Lu¹

¹Dalian University of Technology

²City University of Hong Kong

{kangben, gengwanting, binzhang}@mail.dlut.edu.cn, xche32@cityu.edu.hk

luzhangdut@gmail.com, {zj982853200, wdice, lhchuan}@dlut.edu.cn

Abstract

With growing real-world demands, efficient tracking has received increasing attention. However, most existing methods are limited to RGB inputs and struggle in multi-modal scenarios. Moreover, current multi-modal tracking approaches typically use complex designs, making them too heavy and slow for resource-constrained deployment. To tackle these limitations, we propose **UETTrack**, an efficient framework for single object tracking. UETTrack demonstrates high practicality and versatility, efficiently handling multiple modalities including RGB, Depth, Thermal, Event, and Language, and addresses the gap in efficient multi-modal tracking. It introduces two key components: a Token-Pooling-based Mixture-of-Experts mechanism that enhances modeling capacity through feature aggregation and expert specialization, and a Target-aware Adaptive Distillation strategy that selectively performs distillation based on sample characteristics, reducing redundant supervision and improving performance. Extensive experiments on 12 benchmarks across 3 hardware platforms show that UETTrack achieves a superior speed-accuracy trade-off compared to previous methods. For instance, UETTrack-B achieves 69.2% AUC on LaSOT and runs at 163/56/60 FPS on GPU/CPU/AGX, demonstrating strong practicality and versatility. Code is available at <https://github.com/kangben258/UETTrack>.

1. Introduction

Single Object Tracking (SOT) is a fundamental task in computer vision that aims to continuously locate a specified target in a video. Recently, efficient trackers have gained increasing attention due to their higher practicality compared with mainstream trackers [1, 18, 20, 22, 34, 53, 76, 88, 100]. However, most existing efficient trackers [19, 41, 99] are restricted to RGB-only scenarios, and little effort has been

*Corresponding author.

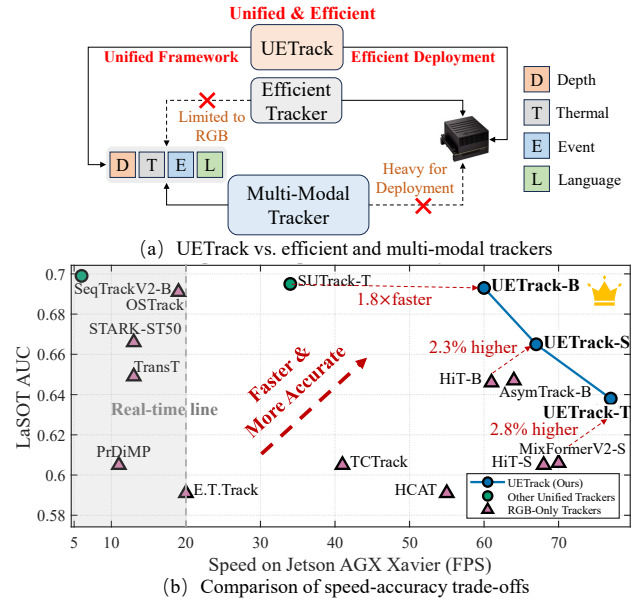


Figure 1. UETTrack vs. Other Trackers. (a) compares UETTrack with current efficient and multi-modal trackers; (b) presents a comparison of speed-accuracy trade-offs on the Jetson AGX.

devoted to efficient multi-modal tracking. In complex real-world environments, a single modality is often insufficient. To enhance robustness, additional modalities such as depth, thermal, or event data are needed. Although several studies [14, 36, 37] have explored multi-modal tracking, the heterogeneity among modalities makes it challenging to effectively capture complementary information and shared representations. Consequently, existing methods often depend on complex designs and large model structures, resulting in high computational cost and latency that hinder their deployment in real-world applications. These limitations raise a key question: *Can we design an efficient multi-modal tracking model suitable for real-world scenarios?*

To address the above issues, we propose an efficient SOT framework named **UETTrack**. As shown in Figure 1(a), UETTrack adopts a lightweight architecture and supports mul-

multiple modalities, including RGB, Depth, Thermal, Event, and Language. This design enables efficient multi-modal tracking with strong practicality and versatility, making UETrack suitable for real-world applications. We follow SUTrack [14] to achieve unified modeling across multiple modalities. Specifically, for depth, thermal, and event data, we concatenate each with the paired RGB image to form a 6-channel composite input, which is fed into a patch embedding layer to generate image token embeddings. For language data, we leverage CLIP [71] to obtain language token embeddings. All embeddings are then jointly processed by the transformer blocks. This unified processing pipeline significantly reduces the computational cost of multi-modal modeling and enables efficient inference across all modalities. Due to the heterogeneity among different modalities, efficient trackers with limited parameters often struggle to capture complementary information and shared representations across modalities. To address this issue, we introduce a Token-Pooling-based Mixture-of-Experts (TP-MoE) structure. Unlike traditional MoE methods [48], TP-MoE eliminates the complex and time-consuming gating mechanism, and instead adopts a soft assignment strategy via weighted feature aggregation. This design enables efficient collaboration and specialization among experts, improving feature modeling in multi-modal scenarios while maintaining high model efficiency. Additionally, we propose a Target-aware Adaptive Distillation (TAD) strategy to further enhance UETrack’s performance. TAD adaptively determines whether a sample requires supervision from the teacher model’s target distributions and feature maps, and dynamically adjusts the degree of distillation. This mechanism filters out misleading signals, mitigating the negative impact of unreliable teacher outputs on the student.

Extensive experiments on 12 datasets and 3 platforms show that UETrack achieves a superior speed-accuracy trade-off across multiple tasks. As shown in Figure 1(b), UETrack-B runs $1.8\times$ faster on AGX and $2.4\times$ faster on CPU than SUTrack-T [14], while maintaining comparable accuracy. UETrack-S improves the AUC on LaSOT by 2.3% and runs $1.1\times$ faster on AGX compared to HiT-B [41]. Similarly, UETrack-T achieves a 2.8% AUC gain on LaSOT over MixFormerV2-S [19], with a $1.1\times$ speedup on AGX. Our contributions are summarized as follows:

- We propose an efficient SOT framework, UETrack, which can efficiently process RGB, Depth, Thermal, Event, and Language modalities. UETrack demonstrates strong practicality and versatility, filling the gap in efficient multi-modal tracking.
- We introduce the Token-Pooling-based Mixture-of-Experts (TP-MoE) to enhance the representation ability for multi-modal inputs. Additionally, we propose the Target-aware Adaptive Distillation (TAD) strategy to further boost performance.

2. Related Work

Efficient Object Tracking. Unlike mainstream deep trackers [30, 55, 57, 64] that prioritize accuracy, efficient trackers aim to balance accuracy and inference speed. Early works [15, 21, 90] are CNN-based [33, 46] and achieve high speed, but their accuracy lags behind mainstream models. With the rise of Transformer architectures [23, 59], several Transformer-based efficient trackers [3, 4, 7, 11, 31, 41, 84, 103] have emerged, significantly improving tracking accuracy while maintaining fast inference. However, most efficient trackers are limited to RGB-only scenarios and underperform in complex environments requiring multi-modal cues. In contrast, our proposed UETrack is a unified framework that supports five modalities, offering improved practicality and versatility.

Multi-Modal Object Tracking. The dominant types of multi-modal tracking include Depth [58, 70], Thermal [87, 95], Event [17, 66], and Language [32, 61]. By leveraging complementary information from auxiliary modalities, these methods significantly improve performance under challenging conditions. Recently, unified modeling has emerged, aiming to handle multiple modalities within a single architecture. Models like ViPT [102], Un-Track [86], SDSTrack [37], and OneTracker [36] adapt existing RGB trackers by incorporating modality-specific modules, while SUTrack [14] uses unified tokens to process multiple modalities without extra modules. However, most of them suffer from complex architectures and high computational cost, limiting practical use. In contrast, our UETrack maintains strong performance with significantly faster inference, offering improved practicality and efficiency.

Knowledge Distillation. Knowledge distillation is a common approach to improve efficient model performance. Existing methods include soft distribution distillation [35, 75], guiding the student to mimic the teacher’s output distribution; feature-based distillation [74, 94], aligning intermediate representations; and relational distillation [67, 80], modeling inter-sample relationships. Recently, adaptive strategies [77, 97] have gained attention for dynamically reducing redundant supervision and enhancing distillation. In this work, we propose a Target-aware Adaptive Distillation strategy tailored for object tracking, improving the specificity and effectiveness of knowledge transfer.

Mixture of Experts (MoE). MoE has emerged as an effective way to expand model capacity while improving computational efficiency, widely adopted in NLP [24, 27]. Recently, MoE extended to vision tasks [69, 73], where learnable routing integrates into ViT to balance modeling power and efficiency. In tracking, methods like MoETrack [78], eMoE-Tracker [16], and SPMTrack [5] leverage MoE to boost performance. However, gating in MOE often introduces latency. To address this, we propose a Token-Pooling-based MoE that eliminates gating for efficient tracking.

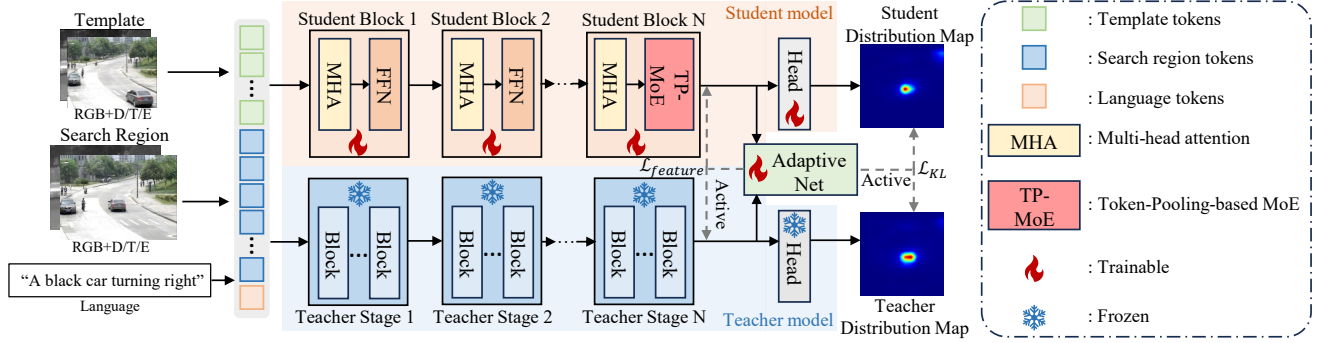


Figure 2. Architecture of UETrack. The training pipeline consists of a teacher model, a student model, and an Adaptive Net for adaptive distillation. During inference, only the student model is used, with TP-MoE as the core component to enhance multi-modal modeling.

3. UETrack

3.1. Overall Architecture

The overall architecture of UETrack is illustrated in Figure 2. We first build an efficient student model based on Token-Pooling-based Mixture-of-Experts (TP-MoE). To enhance its performance, we further propose a Target-aware Adaptive Distillation (TAD) framework, which uses SUTrack-B [14] as the teacher model and incorporates an Adaptive Net to enable dynamic supervision. During training, only the student and Adaptive Net are updated, while the teacher remains frozen.

The input to UETrack consists of multiple modalities, including RGB, Depth, Thermal, Event, and Language. To enable efficient multi-modal modeling, we follow the design of SUTrack by encoding different modalities into unified token embeddings, which minimizes parameter redundancy and computational cost. Specifically, for Depth, Thermal, and Event modalities, the input is formed as an RGB-X image pair, consisting of the original RGB image $\mathbf{I}_{\text{rgb}} \in \mathbb{R}^{H \times W \times 3}$ (H and W denote the height and width of the image) and an auxiliary modality image $\mathbf{I}_{\text{aux}} \in \mathbb{R}^{H \times W \times 3}$. These two images are concatenated along the channel dimension to create a composite image $\mathbf{I}_{\text{c}} \in \mathbb{R}^{H \times W \times 6}$. For RGB and Language modalities, which lack corresponding auxiliary images, we replicate the RGB image along the channel dimension to construct \mathbf{I}_{c} . The template and search images form $\mathbf{I}_{\text{c}}^z \in \mathbb{R}^{H_z \times W_z \times 6}$ and $\mathbf{I}_{\text{c}}^x \in \mathbb{R}^{H_x \times W_x \times 6}$, respectively. These are passed through a patch embedding layer to produce token embeddings $\mathbf{T}_{\text{c}}^z \in \mathbb{R}^{D \times \frac{H_z}{16} \times \frac{W_z}{16}}$ and $\mathbf{T}_{\text{c}}^x \in \mathbb{R}^{D \times \frac{H_x}{16} \times \frac{W_x}{16}}$. The patch embedding process includes a convolutional down-sampling layer with stride 4, followed by MLP layers and two convolutional merging layers to construct high-quality token representations. For the language modality, textual information is extracted using a pre-trained CLIP text encoder [71], which outputs language token embeddings \mathbf{T}_l . These embeddings are projected to match the image token

dimension via a linear transformation. The CLIP encoder remains frozen during training. Finally, the token embeddings \mathbf{T}_{c}^z , \mathbf{T}_{c}^x , and \mathbf{T}_l are concatenated to form the input sequence $\mathbf{T} \in \mathbb{R}^{L \times D}$ ($L = \frac{H_z}{16} \times \frac{W_z}{16} + \frac{H_x}{16} \times \frac{W_x}{16} + 1$).

The input sequence \mathbf{T} is fed into the backbones of both the student and teacher networks for feature extraction. Each backbone consists of a series of transformer blocks. In the student model, several feed-forward networks (FFNs) within these blocks are replaced by Token-Pooling-based MoE modules, which strengthen the student’s modeling capacity through expert collaboration and specialization. After passing through the backbones, we obtain the student features \mathbf{F}_s and teacher features \mathbf{F}_t . These features are further processed by their respective prediction heads to generate the final tracking results. In addition, \mathbf{F}_s and \mathbf{F}_t are input to the Adaptive Net, which decides whether to use the teacher features \mathbf{F}_t and the target distribution to supervise the student. This adaptive strategy prevents redundant or misleading distillation signals, improving both training efficiency and stability.

3.2. Token-Pooling-based MoE

Due to the strong heterogeneity among multi-modal data, models with limited parameters often struggle to learn shared and complementary representations across modalities, which limits their modeling capability. To improve the feature extraction ability of efficient models in such scenarios, we propose a sparse expert mechanism based on token aggregation, called Token-Pooling-based Mixture-of-Experts (TP-MoE). Unlike traditional MoE models that use discrete gating functions for token routing, TP-MoE adopts a similarity-driven soft assignment strategy. It measures the similarity between input tokens and expert tokens and performs weighted aggregation to enable adaptive collaboration among experts.

As shown in Figure 3, TP-MoE first enhances short-range dependency modeling through a local aggregation module. Specifically, the input tokens $\mathbf{T}_{\text{in}} \in \mathbb{R}^{L_1 \times D}$ (L_1

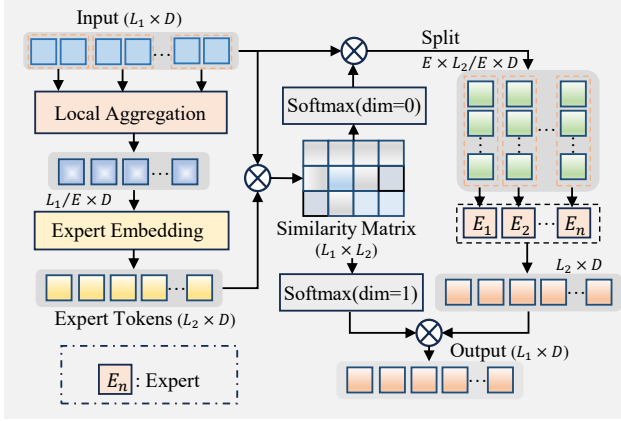


Figure 3. TP-MoE architecture diagram.

denotes the length of the input) are divided into L_1/E subspaces, where E denotes the number of experts, and average pooling is applied within each subspace. This operation strengthens local contextual relationships while preserving structural consistency among nearby tokens. Next, the aggregated tokens are transformed into compact expert tokens $\mathbf{T}_e \in \mathbb{R}^{L_2 \times D}$ (L_2 denotes the length of expert tokens) through an expert embedding module, which consists of a linear projection followed by a reshape operation. A similarity matrix $\mathbf{S} \in \mathbb{R}^{L_1 \times L_2}$ is then computed between the input and expert tokens, and a softmax along the first dimension produces the routing weights \mathbf{S}_a . These weights acts as a continuous routing map, enabling efficient and fully parallel token–expert interactions. Instead of relying on explicit gating or discrete routing, TP-MoE performs similarity-based soft weighting through matrix multiplication. The routing weights \mathbf{S}_a determine how much each input token contributes to each expert, where higher similarity results in larger weights and stronger influence. Based on \mathbf{S}_a , the input tokens are softly aggregated and sequentially grouped to form the expert inputs $\mathbf{T}_a \in \mathbb{R}^{E \times \frac{L_2}{E} \times D}$. \mathbf{T}_a contains E expert groups, each with L_2/E subspace tokens, ensuring that every expert focuses on distinct semantic regions. Each expert independently processes its input to generate the expert outputs $\mathbf{O}_e \in \mathbb{R}^{L_2 \times D}$. Finally, these outputs are aggregated back to the input token space through another softmax weighting over the similarity matrix \mathbf{S} , yielding a refined and more discriminative representation $\mathbf{O} \in \mathbb{R}^{L_1 \times D}$. The entire process is summarized as follows:

$$\begin{aligned}
 \mathbf{T}_e &= \text{Embed}(\text{Aggre}(\mathbf{T}_{\text{in}})) \\
 \mathbf{T}_a &= \text{Split}(\text{Softmax}(\mathbf{T}_{\text{in}} \mathbf{T}_e^\top)^\top \mathbf{T}_{\text{in}}) \\
 \mathbf{O}_e &= \text{Merge} \left(\left\{ \text{Expert}_i(\mathbf{T}_a^i) \right\}_{i=1}^E \right) \\
 \mathbf{O} &= \text{Softmax}(\mathbf{T}_{\text{in}} \mathbf{T}_e^\top) \mathbf{O}_e
 \end{aligned} \tag{1}$$

where \mathbf{T}_a^i is the input to the i -th expert. $\text{Aggre}(\cdot)$ refers

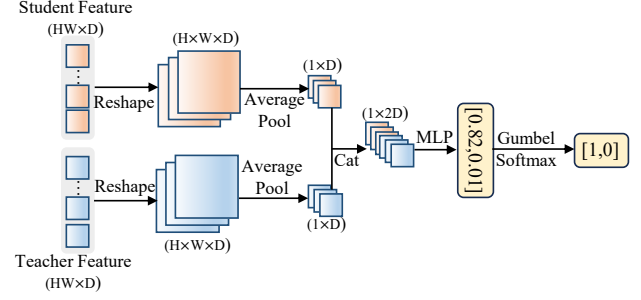


Figure 4. Architecture of Adaptive Net.

to the local aggregation, $\text{Embed}(\cdot)$ is the expert embedding module, $\text{Softmax}(\cdot)$ denotes the softmax activation, $\text{Split}(\cdot)$ denotes sequentially partitioning tokens according to the number of experts, $\text{Expert}_i(\cdot)$ represents the i -th expert, and $\text{Merge}(\cdot)$ merges the outputs from all experts.

This attention-like assignment strategy can be interpreted as a subspace projection that maps input tokens onto multiple expert manifolds, where each expert focuses on the inputs most relevant to its own subspace to capture complementary semantics within a shared feature space. This mechanism encourages subspace specialization and feature diversity, thereby mitigating modality heterogeneity and enhancing representation quality. Meanwhile, the continuous routing design supports fully parallel computation and removes the overhead of hard gating, such as token sorting and inter-expert communication. The differentiable matrix operation also stabilizes gradient propagation, resulting in lower latency and improved training stability, which is desirable for real-time visual tracking. Through explicit local aggregation, lightweight expert embedding, and parallel soft-assignment, TP-MoE enables efficient collaboration and specialization among experts without requiring additional gating parameters or cross-expert communication. This mechanism effectively improves the model’s representation capability. It can be flexibly integrated into the backbone by replacing the feed-forward module in transformer blocks, thus improving the model’s ability to extract and fuse multi-modal features.

3.3. Target-aware Adaptive Distillation

To further enhance model performance, we propose a distillation strategy called Target-aware Adaptive Distillation (TAD). Specifically, after the center head, the model outputs a probability distribution map of the target’s center location. The teacher’s distribution map serves as a supervisory signal to guide the student via soft imitation, minimizing the divergence between the teacher and student. This encourages more accurate predictions. Additionally, feature maps from the teacher’s backbone provide auxiliary supervision to further improve the student’s ability to replicate the teacher’s representations.

However, for challenging samples such as those affected by occlusion, distractions, or deformation, the teacher model’s predictions may not be reliable. Directly applying distillation in these cases can transfer incorrect information to the student, introducing noisy supervision and reducing learning effectiveness. Therefore, it is necessary to prevent unreliable teacher guidance on such difficult samples to preserve the student’s learning quality on more trustworthy ones. To address this, TAD incorporates an adaptive distillation mechanism that automatically determines whether a given sample is suitable for distillation based on its features. The core of this mechanism is the Adaptive Net, illustrated in Figure 4. It takes as input the search region feature sequence \mathbf{T}_s from the student and \mathbf{T}_t from the teacher. Both \mathbf{T}_t and \mathbf{T}_s are reshaped into 3D tensors and passed through global average pooling. The pooled features are concatenated into a fused vector \mathbf{T}_c , which is then fed into an MLP for dimensionality reduction, producing a 2D vector. This vector is converted into a one-hot vector via the Gumbel-Softmax [40] operation and output as \mathbf{O} by the Adaptive Net. The value of \mathbf{O} determines whether the current sample should undergo distillation, enabling fine-grained, sample-level control.

3.4. Training Objective

To ensure stable training, the student and Adaptive Net are updated separately. The student’s training objective combines focal classification loss [47], GIoU [72] and L1 regression losses, cross-entropy task loss [14], and distillation losses based on KL divergence and MSE, as detailed below:

$$\begin{aligned} \mathcal{L}_S = & \mathcal{L}_c(\hat{p}_s, p) + \lambda_g \mathcal{L}_g(\hat{p}_s, p) + \lambda_{l_1} \mathcal{L}_{l_1}(\hat{p}_s, p) \\ & + \mathcal{L}_t(\hat{p}_s, p) + \alpha(\lambda_{kd} \mathcal{L}_{kd}(\hat{p}_s, \hat{p}_t) + \lambda_f \mathcal{L}_f(\hat{p}_s, \hat{p}_t)) \end{aligned} \quad (2)$$

where \mathcal{L}_c , \mathcal{L}_g , \mathcal{L}_{l_1} , \mathcal{L}_t , \mathcal{L}_{kd} , and \mathcal{L}_f denote classification, GIoU, L1, task, KL, and MSE losses, respectively. \hat{p}_s , \hat{p}_t , and p are the student prediction, teacher prediction, and ground truth. Hyperparameters are $\lambda_g = 2$, $\lambda_{l_1} = 5$, $\lambda_{kd} = 5$, and $\lambda_f = 0.002$. α is the Adaptive Net output: $\alpha = 1$ means the sample is distilled; otherwise, $\alpha = 0$.

For the Adaptive Net, we adopt a surrogate prediction strategy. For each sample, it outputs a binary decision indicating whether to perform distillation. Based on this, a surrogate prediction is selected: if distillation is chosen, the teacher’s prediction serves as the target; otherwise, the student’s prediction is used. The surrogate prediction is compared with the ground truth to compute the loss, which mirrors the student’s objective but excludes distillation loss. Details are as follows:

$$\hat{p}_a^i = \begin{cases} \hat{p}_t^i & \text{if } \alpha = 1, \\ \hat{p}_s^i & \text{if } \alpha = 0 \end{cases} \quad (3)$$

$$\mathcal{L}_A = \mathcal{L}_c(\hat{p}_a, p) + \lambda_g \mathcal{L}_g(\hat{p}_a, p) + \lambda_{l_1} \mathcal{L}_{l_1}(\hat{p}_a, p) + \mathcal{L}_t(\hat{p}_a, p) \quad (4)$$

Table 1. Details of UETrack model variants.

Model	Architecture	GPU Speed (fps)	CPU Speed (fps)	AGX Speed (fps)	Params (M)	FLOPs (G)
UETrack-B	[6, [6], 8]	163	56	60	13	3.2
UETrack-S	[4, [4], 4]	183	68	67	9	2.5
UETrack-T	[2, [2], 2]	221	83	77	6	1.8

where \hat{p}_t^i , \hat{p}_s^i , and \hat{p}_a^i denote the teacher, student, and surrogate predictions for the i -th sample, respectively.

4. Experiments

4.1. Implementation Details

Model. UETrack is built on Fast-iTPN-T [79], using its first N layers as the backbone. The prediction head adopts a center head [93]. We develop three UETrack variants, as summarized in Table 1. In the Architecture column, $[i, [j], k]$ indicates that the backbone has i layers, TP-MoE is inserted at the j -th layer, and k experts are used. For instance, UETrack-B uses the first 6 layers of Fast-iTPN-T as the backbone, with TP-MoE at the 6th layer and 8 experts. Table 1 also reports the inference speed on 2080Ti GPU, Intel i9-14900KF CPU, and Jetson AGX Xavier, as well as model parameters and FLOPs. All models are implemented in Python 3.8.13 and PyTorch 1.13.1.

Training. We construct the training dataset by combining data from five common modalities, including COCO [54], LaSOT [25], GOT-10k [38], TrackingNet [65], VAST-Track [68], DepthTrack [91], VisEvent [83], LasHeR [50], OTB99 [52], and TNL2K [82]. During training, we use RGB-X image pairs as inputs for both the template and search region, with resolutions of 224×224 and 112×112 , respectively. The template and search images are generated by enlarging the bounding boxes by a factor of 2 and 4. Data augmentation includes horizontal flipping and brightness jittering. The backbone parameters are initialized with a pretrained Fast-iTPN-T model, while the remaining ones are randomly initialized. We use the AdamW [60] optimizer with an initial learning rate of 1×10^{-5} for the backbone and 1×10^{-4} for the rest. The weight decay is set to 1×10^{-4} . The model is trained for 500 epochs, with 100,000 samples per epoch. The learning rate is reduced by a factor of 10 after epoch 400. Training is conducted on two 80GB Tesla A800 GPUs with a total batch size of 128.

Inference. During inference, only the student is used. To incorporate positional priors, a Hanning window penalty is applied, following standard tracking practices [93].

4.2. State-of-the-Art Comparisons

We conduct a comprehensive comparison between UETrack and state-of-the-art methods across five modalities, twelve datasets, and three different hardware platforms. A tracker is defined as real-time if it runs over 20 FPS on the Jetson AGX Xavier; otherwise, it is considered non-real-time.

Table 2. State-of-the-art (SOTA) comparisons on four large-scale RGB benchmarks. The top three real-time results are highlight with **red**, **blue** and **green** fonts, respectively. The top three speed across different platforms are highlighted in **bold**.

	Method	LaSOT			LaSOT _{ext}			TrackingNet			GOT-10k			Speed (fps)		
		AUC	P _{Norm}	P	AUC	P _{Norm}	P	AUC	P _{Norm}	P	AO	SR _{0.5}	SR _{0.75}	GPU	CPU	AGX
Real-time	UETTrack-B (Ours)	69.2	78.4	73.8	48.4	59.0	54.5	82.7	87.4	80.7	72.6	82.5	69.8	163	56	60
	UETTrack-S (Ours)	66.9	76.1	70.7	47.9	58.4	53.9	81.4	86.3	78.8	71.1	81.2	67.0	183	68	67
	UETTrack-T (Ours)	63.4	72.5	65.1	42.2	51.5	46.1	78.9	83.8	74.8	65.3	75.1	58.4	221	83	77
	AsymTrack-B [103]	64.7	73.0	67.8	44.6	-	-	80.0	84.5	77.4	67.7	76.6	61.4	197	38	64
	DyHiT [43]	62.4	70.1	64.0	42.1	-	-	77.9	82.2	73.8	62.9	71.8	55.2	299	63	111
	HiT-Base [41]	64.6	73.3	68.1	44.1	-	-	80.0	84.4	77.3	64.0	72.1	58.1	175	33	61
	MixFormerV2-S [19]	60.6	69.9	60.4	43.6	-	46.2	75.8	81.1	70.4	61.9	71.7	51.3	299	47	70
	TCTrack [8]	60.5	69.3	62.4	-	-	-	74.8	79.6	73.3	66.2	75.6	61.0	140	45	41
	FEAR [4]	53.5	-	54.5	-	-	-	-	-	-	61.9	72.2	-	105	60	38
	HCAT [11]	59.3	68.7	61.0	40.6	-	-	76.6	82.6	72.9	65.1	76.5	56.7	195	45	55
	E.T.Track [3]	59.1	-	-	-	-	-	75.0	80.3	70.6	-	-	-	40	47	20
	LightTrack [90]	53.8	-	53.7	-	-	-	72.5	77.8	69.5	61.1	71.0	-	128	41	36
	ATOM [21]	51.5	57.6	50.5	37.6	45.9	43.0	70.3	77.1	64.8	55.6	63.4	40.2	83	18	22
Non-real-time	MCITrack-B224 [42]	75.3	85.6	83.3	54.6	65.7	62.1	86.3	90.9	86.1	77.9	88.2	76.8	34	2	6
	SUTrack-B224 [14]	73.2	83.4	80.5	53.1	64.2	60.5	85.7	90.3	85.1	77.9	87.5	78.5	55	6	13
	MixFormerV2-B [19]	70.6	80.8	76.2	50.6	-	56.9	83.4	88.1	81.6	73.9	-	-	116	11	16
	SeqTrack-B256 [12]	69.9	79.7	76.3	49.5	60.8	56.3	83.3	88.3	82.2	74.7	84.7	71.8	31	2	6
	ARTrack-256 [85]	70.4	79.5	76.6	46.4	56.5	52.3	84.2	88.7	83.5	73.5	82.2	70.9	39	3	6
	OStTrack-256 [93]	69.1	78.7	75.2	47.4	57.3	53.3	83.1	87.8	82.0	71.0	80.4	68.2	105	11	19
	Sim-B/16 [9]	69.3	78.5	-	-	-	-	82.3	86.5	-	68.6	78.9	62.4	87	10	16
	STARK-ST50 [89]	66.6	-	-	-	-	-	81.3	86.1	-	68.0	77.7	62.3	50	7	13
	TransT [10]	64.9	73.8	69.0	44.4	-	-	81.4	86.7	83.0	67.1	76.8	60.9	63	5	13
	DiMP [2]	56.9	65.0	56.7	39.2	47.6	45.1	74.0	80.1	68.7	61.1	71.7	49.2	77	10	17

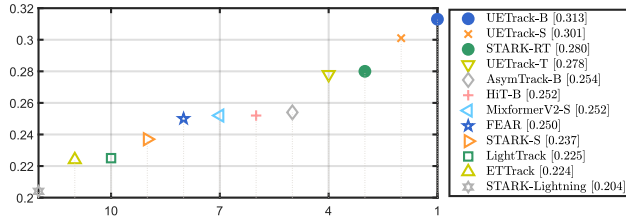


Figure 5. EAO rank plots on VOT2021 Real-time.

RGB-based Tracking. We evaluate UETTrack on five RGB benchmarks, including LaSOT [25], LaSOT_{ext} [26], TrackingNet [65], GOT-10k [38], and VOT2021 Real-time [44]. The evaluation results are summarized in Table 2 and Figure 5. As shown, UETTrack-B and UETTrack-S achieve top-2 performance across all five benchmarks compared to previous real-time trackers. Specifically, UETTrack-B obtains AUC scores of 69.2%, 48.4%, and 82.7% on LaSOT, LaSOT_{ext}, and TrackingNet, respectively; an AO score of 72.6% on GOT-10k; and an EAO score of 0.313 on the VOT2021 Real-time. These results outperform the previous best real-time tracker, AsymTrack [103], by margins of 4.5%, 3.8%, 2.7%, 4.9%, and 0.059, respectively, setting a new state-of-the-art for real-time tracking. Notably, compared to OStTrack [93], UETTrack-B achieves higher scores on LaSOT (+0.1%), LaSOT_{ext} (+1.0%), and GOT-10k (+1.6%), while running significantly faster—1.6× on GPU, 5.1× on CPU, and 3.2× on AGX.

RGB-Depth Tracking. UETTrack delivers strong perfor-

Table 3. SOTA comparisons on depth modality.

	Method	VOT-RGBD22		DepthTrack		Speed (fps)		
		EAO	Acc.	F-score	Re	GPU	CPU	AGX
Real-time	UETTrack-B (Ours)	68.3	80.8	60.6	61.0	163	56	60
	UETTrack-S (Ours)	66.5	79.9	58.9	58.0	183	68	67
	UETTrack-T (Ours)	62.5	77.4	55.7	54.8	221	83	77
	SUTrack-T [14]	68.1	81.0	61.7	62.1	100	23	34
	EMTrack [56]	69.7	80.6	58.3	58.5	109	29	36
	CMDTrack-T9 [96]	-	-	58.1	59.3	145	51	58
Non-real-time	ViPT-Tiny [56]	68.5	80.4	53.9	53.7	56	22	20
	SeqTrackv2 [13]	74.4	81.5	63.2	63.4	23	2	5
	OneTracker [36]	72.7	81.9	60.9	60.4	-	-	-
	SDSTrack [37]	72.8	81.2	61.9	60.9	42	3	7
	Un-Track [86]	72.1	82.0	61.0	60.8	22	4	5
	ViPT [102]	72.1	81.5	59.4	59.6	55	6	13
	OStTrack [93]	67.6	80.3	52.9	52.2	105	11	19
	SPT [104]	65.1	79.8	53.8	54.9	25	-	-
	DeT [91]	65.7	76.0	53.2	50.6	37	-	-

mance on RGB-Depth tasks while maintaining high inference speed. As shown in Table 3, on the VOT-RGBD22 benchmark [45], UETTrack-B achieves an EAO of 68.3%, surpassing SUTrack-T by 0.2%, and runs 1.6×, 2.4×, and 1.8× faster on GPU, CPU, and AGX, respectively. On DepthTrack [91], UETTrack-B achieves an F-score of 60.6%. It outperforms EMTrack by 2.3%, with speed gains of 1.5×, 1.9×, and 1.7× on GPU, CPU, and AGX, respectively. Compared to ViPT, UETTrack-B achieves a 1.2% higher F-score, and runs 3.0×, 9.3×, and 4.6× faster on GPU, CPU, and AGX, respectively.

Table 4. SOTA comparisons on thermal modality.

	Method	LasHeR		RGBT234		Speed (fps)		
		AUC	P	MSR	MPR	GPU	CPU	AGX
Real-time	UETrack-B (Ours)	55.5	69.1	64.2	86.7	163	56	60
	UETrack-S (Ours)	53.2	66.4	62.2	84.4	183	68	67
	UETrack-T (Ours)	48.2	59.8	59.3	81.3	221	83	77
	SUTrack-T [14]	53.9	66.7	63.8	85.9	100	23	34
	EMTrack [56]	53.3	65.9	60.1	81.8	109	29	36
	CMDTrack-T9 [96]	52.8	65.4	59.8	83.1	145	51	58
ViPT-Tiny [56]	47.5	58.5	58.8	80.0	56	22	20	
Non-real-time	SeqTrackv2 [13]	55.8	70.4	64.7	88.0	23	2	5
	OneTracker [36]	53.8	67.2	64.2	85.7	-	-	-
	SDSTrack [37]	53.1	66.5	62.5	84.8	42	3	7
	Un-Track [86]	51.3	54.6	62.5	84.2	22	4	5
	ViPT [102]	52.5	65.1	61.7	83.5	55	6	13
	ProTrack [92]	42.0	53.8	59.9	79.5	-	-	-
	BAT [6]	56.3	70.2	64.1	86.8	56	3	7
	TBSI [39]	55.6	69.2	63.7	87.1	42	2	5
	TATrack [81]	56.1	70.2	64.4	87.2	26	-	-

Table 5. SOTA comparisons on event modality.

	Method	VisEvent		Speed (fps)		
		AUC	P	GPU	CPU	AGX
Real-time	UETrack-B (Ours)	59.2	76.2	163	56	60
	UETrack-S (Ours)	58.0	75.1	183	68	67
	UETrack-T (Ours)	54.4	71.8	221	83	77
	SUTrack-T [14]	58.8	75.7	100	23	34
	EMTrack [56]	58.4	72.4	109	29	36
	CMDTrack-T9 [96]	57.9	72.4	145	51	58
ViPT-Tiny [56]	55.8	69.8	56	22	20	
Non-real-time	SeqTrackv2 [13]	61.2	78.2	23	2	5
	OneTracker [36]	60.8	76.7	-	-	-
	SDSTrack [37]	59.7	76.7	42	3	7
	Un-Track [86]	58.9	75.5	22	4	5
	ViPT [102]	59.2	75.8	55	6	13
	ProTrack [92]	47.1	63.2	-	-	-
	OStTrack [93]	53.4	69.5	105	11	19

RGB-Thermal Tracking. UETrack achieves best real-time performance on LasHeR [50] and RGBT234 [49], as shown in Table 4. UETrack-B records 55.5% AUC on LasHeR and 64.2% MSR on RGBT234, surpassing SUTrack-T by 1.6% and 0.4%, respectively. Compared to the non-real-time SDSTrack, UETrack-B improves by 2.4% on LasHeR and 1.7% on RGBT234, while running 3.9 \times , 18.7 \times , and 8.6 \times faster on GPU, CPU, and AGX, respectively.

RGB-Event Tracking. As shown in Table 5, UETrack achieves a new real-time state-of-the-art on VisEvent [83]. Specifically, UETrack-B obtains an AUC score of 59.2%, surpassing the previous real-time trackers SUTrack-T and EMTrack by 0.4% and 0.8%, respectively.

RGB-Language Tracking. UETrack also demonstrates competitive performance on the Language modality. As shown in Table 6, UETrack-B achieves an AUC score of 58.0% on TNL2K [82], surpassing SeqTrackv2 by 0.5%,

Table 6. SOTA comparisons on language modality.

	Method	TNL2K		OTB99		Speed (fps)		
		AUC	P	AUC	P	GPU	CPU	AGX
Real-time	UETrack-B (Ours)	58.0	60.3	61.3	79.7	163	56	60
	UETrack-S (Ours)	57.0	58.4	63.1	81.9	183	68	67
	UETrack-T (Ours)	54.4	54.4	64.8	84.7	221	83	77
	SUTrack-T [14]	60.9	62.3	67.4	88.6	100	23	34
Non-real-time	SeqTrackv2 [13]	57.5	59.7	71.2	93.9	23	2	5
	OneTracker [36]	58.0	59.1	69.7	91.5	-	-	-
	UVLTrack-B [63]	63.1	66.7	69.3	89.9	52	4	6
	CiteTracker [51]	57.7	59.6	69.6	85.1	22	2	4
	JointNLT [101]	56.9	58.1	65.3	85.6	39	3	5
	DecoupleTNL [62]	56.7	56.0	73.8	94.8	32	-	-
	Zhao <i>et al.</i> [98]	56.0	-	69.9	91.2	36	-	-
	SNLT [29]	27.6	41.9	66.6	80.4	50	-	-
RTTNLD [28]	25.0	27.0	61.0	79.0	30	-	-	

Table 7. Ablation Study. Δ denotes the performance change (averaged over benchmarks) compared with the baseline. The speed is measured on the AGX.

#	Method	LaSOT	DepthTrack	RGBT234	VisEvent	TNL2K	Speed	Δ
1	Baseline	68.5	59.4	63.1	57.9	57.1	60	-
2	W/o TP-MoE	67.9	58.1	62.2	57.3	56.4	63	-0.8
3	Gate-MoE	68.7	59.1	62.9	57.6	56.7	39	-0.2
4	W/o Local Agg.	68.0	59.3	63.2	57.0	56.8	61	-0.3
5	4 Experts	68.0	59.5	62.4	57.4	56.7	60	-0.4
6	16 Experts	68.2	58.6	62.2	57.5	56.6	60	-0.6
7	32 Experts	68.5	59.3	62.4	57.1	56.4	59	-0.5
8	Last 2 Layers	67.7	59.3	63.2	57.6	57.2	53	-0.2
9	Last 3 Layers	67.5	58.1	62.7	57.3	57.4	48	-0.6
10	Even Layers	67.2	59.2	62.2	57.5	57.0	48	-0.6
11	+ KL	68.7	59.7	63.7	58.0	57.2	60	+0.3
12	+ Feature Mim.	69.0	60.1	63.7	58.2	57.4	60	+0.5
13	+ Adaptive	69.2	60.6	64.2	59.2	58.0	60	+1.0

while running 7.1 \times , 28 \times , and 12 \times faster on GPU, CPU, and AGX, respectively. On OTB99 [52], UETrack-B, UETrack-S, and UETrack-T achieve AUC scores of 61.3%, 63.1%, and 64.8%, respectively.

Speed comparison. We compare the tracking speed on three platforms. UETrack consistently achieves better speed-accuracy trade-offs than previous trackers. For example, the fastest variant, UETrack-T, runs at 221 FPS on GPU, 83 FPS on CPU, and 77 FPS on AGX, outperforming most RGB-only trackers. In RGB-X tasks, multi-modal processing typically introduces extra latency, slowing down existing trackers. However, UETrack significantly boosts multi-modal tracking speed. Compared to the unified SUTrack-T, UETrack-T achieves 2.2 \times , 3.6 \times , and 2.3 \times higher speed on GPU, CPU, and AGX, respectively. Overall, UETrack runs fast on all three platforms and supports five modalities, validating its practicality and versatility.

4.3. Ablation and Analysis

As shown in Table 7, we conduct extensive ablation experiments to validate the effectiveness of the proposed TP-MoE

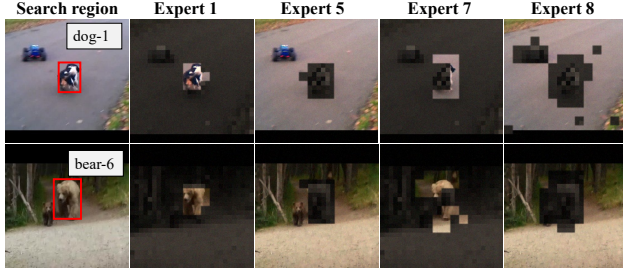


Figure 6. Visualization of attention distributions of TP-MoE experts. The bright regions denote the attended areas. Each expert focuses on distinct spatial regions.

and TAD. In Table 7, models #1 to #10 are all trained without TAD. The baseline model (#1) is UETTrack-B, which incorporates TP-MoE but does not use TAD.

Necessity of TP-MoE. To verify the effectiveness of TP-MoE, we conduct three groups of experiments. In #2, TP-MoE is entirely removed. In #3, it is replaced by a gated MoE that assigns tokens through a gating mechanism. In #4, the local aggregation process within TP-MoE is removed. As observed, removing TP-MoE (#2) leads to performance drops across multiple datasets, with an average decrease of 0.8%. Replacing TP-MoE with the gated MoE (#3) also causes a slight drop of 0.2% on average. Moreover, due to the time-consuming gating mechanism in the gated MoE, the model speed drops significantly—by 21 FPS compared to the baseline. When the local aggregation is removed (#4), the model shows an average accuracy decrease of 0.3%. These results demonstrate the necessity of TP-MoE. It enhances the model’s ability to process multi-modal inputs, while the similarity-driven soft assignment replaces explicit gating to maintain high efficiency.

Number of Experts. The number of experts used in TP-MoE is a critical parameter. Too few experts can limit the model’s representation capacity, while too many may introduce redundancy. We evaluate this factor by varying the number of experts, as shown in Table 7, entries #5, #6, and #7, where we use 4, 16, and 32 experts, respectively. The baseline model uses 8 experts by default. As the results show, using 4, 16, and 32 experts leads to average performance drops of 0.4%, 0.6%, and 0.5%, respectively.

Insertion Layer of TP-MoE. We further explore where to insert TP-MoE within the backbone. As shown in Table 7, entries #8, #9, and #10 correspond to inserting TP-MoE in the last two layers, the last three layers, and all even-numbered layers, respectively. The baseline model inserts TP-MoE only in the last layer. The results show that inserting TP-MoE in the last two layers, last three layers, and even-numbered layers leads to average performance drops of 0.2%, 0.6%, and 0.6%, respectively. We attribute this to the fact that semantic features in the deeper layers are more stable and abstract, making them more suitable for expert specialization. In contrast, inserting TP-MoE into earlier

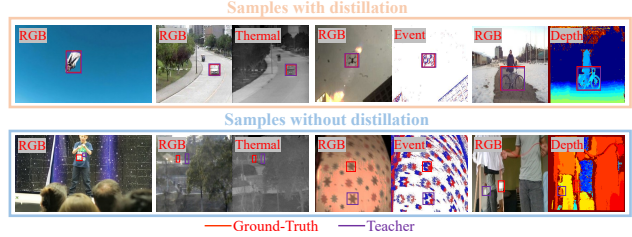


Figure 7. Visualization of adaptive distillation decisions made by TAD across different modalities.

layers may disrupt the still-forming feature representations, causing interference and performance degradation.

Effectiveness of TAD. To validate the effectiveness of the proposed TAD, we perform ablation studies on its individual components. As shown in Table 7, entry #11 introduces KL divergence supervision based on the target distribution. Entry #12 further adds feature-level supervision, and entry #13 incorporates adaptive distillation. The results show that introducing KL divergence improves average performance by 0.3%. Adding feature distillation further increases the gain to 0.5%. Finally, incorporating adaptive distillation leads to a total improvement of 1.0% over the baseline. These results demonstrate the effectiveness of TAD in efficiently transferring knowledge from teacher to student.

Visualization. We visualize the attention distributions of several experts in TP-MoE, as shown in Figure 6. Each expert focuses on different regions. Specifically, Expert 1 attends to the object center, Expert 5 and Expert 8 focus on the background, while Expert 7 concentrates on the object contour. Such collaboration and clear division of attention enable experts to learn complementary representations, thereby enhancing the model’s feature modeling capability. We also visualize the distillation decisions of TAD, as shown in Figure 7. When the scene contains challenges such as blur, occlusion, or deformation, the teacher model often makes inaccurate predictions, and TAD skips distillation for these unreliable samples. This demonstrates the effectiveness of TAD, as it prevents the student from being misled by incorrect supervision.

5. Conclusion

We propose UETTrack, a unified and efficient tracking framework trained once and deployed across five modality-specific tasks. To improve multi-modal modeling and versatility, UETTrack introduces a Token-Pooling-based MoE module for expert collaboration and a Target-aware Adaptive Distillation strategy to selectively transfer knowledge from teacher models. These designs broaden the scope of efficient trackers while improving speed and practicality in multi-modal tracking. Extensive experiments show UETTrack achieves strong versatility and reliability across scenarios. We hope UETTrack bridges research and real-world use, promoting practical multi-modal tracking.

Acknowledgements The paper is supported in part by National Natural Science Foundations of China (no. U23A20384 and no. 62402084), in part Fundamental Scientific Research Funding of the Central Universities of China (DUTZD25225), Liaoning Provincial Science and Technology Joint Program Project (2024011188-JH2/1026), China Postdoctoral Science Foundation (no. 2024M750319).

References

- [1] Yifan Bai, Zeyang Zhao, Yihong Gong, and Xing Wei. AR-TrackV2: Prompting autoregressive tracker where to look and how to describe. In *CVPR*, pages 19048–19057, 2024. 1
- [2] Goutam Bhat, Martin Danelljan, Luc Van Gool, and Radu Timofte. Learning discriminative model prediction for tracking. In *ICCV*, pages 6182–6191, 2019. 6
- [3] Philippe Blatter, Menelaos Kanakis, Martin Danelljan, and Luc Van Gool. Efficient Visual Tracking with Exemplar Transformers. In *WACV*, pages 1571–1581, 2023. 2, 6
- [4] Vasyl Borsuk, Roman Vei, Orest Kupyn, Tetiana Martyniuk, Igor Krashenyi, and Jiri Matas. FEAR: Fast, Efficient, Accurate and Robust Visual Tracker. In *ECCV*, pages 644–663, 2022. 2, 6
- [5] Wenrui Cai, Qingjie Liu, and Yunhong Wang. Spmtrack: Spatio-temporal parameter-efficient fine-tuning with mixture of experts for scalable visual tracking. In *CVPR*, pages 16871–16881, 2025. 2
- [6] Bing Cao, Junliang Guo, Pengfei Zhu, and Qinghua Hu. Bi-directional adapter for multi-modal tracking. In *AAAI*, pages 927–935, 2024. 7
- [7] Ziang Cao, Changhong Fu, Junjie Ye, Bowen Li, and Yiming Li. Hift: Hierarchical feature transformer for aerial tracking. In *ICCV*, pages 15457–15466, 2021. 2
- [8] Ziang Cao, Ziyuan Huang, Liang Pan, Shiwei Zhang, Ziwei Liu, and Changhong Fu. Tctrack: Temporal contexts for aerial tracking. In *CVPR*, pages 14778–14788, 2022. 6
- [9] Boyu Chen, Peixia Li, Lei Bai, Lei Qiao, Qihong Shen, Bo Li, Weihao Gan, Wei Wu, and Wanli Ouyang. Backbone is all your need: A simplified architecture for visual object tracking. In *ECCV*, pages 375–392, 2022. 6
- [10] Xin Chen, Bin Yan, Jiawen Zhu, Dong Wang, Xiaoyun Yang, and Huchuan Lu. Transformer tracking. In *CVPR*, pages 8126–8135, 2021. 6
- [11] Xin Chen, Ben Kang, Dong Wang, Dongdong Li, and Huchuan Lu. Efficient Visual Tracking via Hierarchical Cross-Attention Transformer. In *ECCVW*, pages 461–477, 2022. 2, 6
- [12] Xin Chen, Houwen Peng, Dong Wang, Huchuan Lu, and Han Hu. Seqtrack: Sequence to sequence learning for visual object tracking. In *CVPR*, pages 14572–14581, 2023. 6
- [13] Xin Chen, Ben Kang, Jiawen Zhu, Dong Wang, Houwen Peng, and Huchuan Lu. Unified sequence-to-sequence learning for single- and multi-modal visual object tracking. *arXiv preprint arXiv:2304.14394*, 2024. 6, 7
- [14] Xin Chen, Ben Kang, Wanting Geng, Jiawen Zhu, Yi Liu, Dong Wang, and Huchuan Lu. Sutrack: Towards simple and unified single object tracking. In *AAAI*, pages 2239–2247, 2025. 1, 2, 3, 5, 6, 7
- [15] Xin Chen, Ben Kang, Jiawen Zhu, Dongdong Li, Chunjuan Bo, and Dong Wang. Exploring a hierarchical cross-attention transformer for high-speed tracking. *CVM*, pages 1113–1132, 2025. 2
- [16] Yucheng Chen and Lin Wang. emoe-tracker: Environmental moe-based transformer for robust event-guided object tracking. *IEEE RAL*, pages 1393–1400, 2024. 2
- [17] Zedu Chen, Bineng Zhong, Guorong Li, Shengping Zhang, and Rongrong Ji. Siamese box adaptive network for visual tracking. In *CVPR*, pages 6668–6677, 2020. 2
- [18] Yutao Cui, Cheng Jiang, Limin Wang, and Gangshan Wu. Mixformer: End-to-end tracking with iterative mixed attention. In *CVPR*, pages 13608–13618, 2022. 1
- [19] Yutao Cui, Tianhui Song, Gangshan Wu, and Limin Wang. Mixformerv2: Efficient fully transformer tracking. In *NeurIPS*, pages 58736–58751, 2023. 1, 2, 6
- [20] Yutao Cui, Cheng Jiang, Limin Wang, and Gangshan Wu. Mixformer: End-to-end tracking with iterative mixed attention. *IEEE TPAMI*, pages 0–18, 2024. 1
- [21] Martin Danelljan, Goutam Bhat, Fahad Shahbaz Khan, and Michael Felsberg. ATOM: Accurate tracking by overlap maximization. In *CVPR*, pages 4660–4669, 2019. 2, 6
- [22] Martin Danelljan, Luc Van Gool, and Radu Timofte. Probabilistic regression for visual tracking. In *CVPR*, pages 7183–7192, 2020. 1
- [23] Alexey Dosovitskiy, Lucas Beyer, Alexander Kolesnikov, Dirk Weissenborn, Xiaohua Zhai, Thomas Unterthiner, Mostafa Dehghani, Matthias Minderer, Georg Heigold, Sylvain Gelly, et al. An image is worth 16x16 words: Transformers for image recognition at scale. In *ICLR*, 2020. 2
- [24] Nan Du, Yanping Huang, Andrew M Dai, Simon Tong, Dmitry Lepikhin, Yuanzhong Xu, Maxim Krikun, Yanqi Zhou, Adams Wei Yu, Orhan Firat, et al. Glam: Efficient scaling of language models with mixture-of-experts. In *ICML*, pages 5547–5569, 2022. 2
- [25] Heng Fan, Liting Lin, Fan Yang, Peng Chu, Ge Deng, Sijia Yu, Hexin Bai, Yong Xu, Chunyuan Liao, and Haibin Ling. LaSOT: A high-quality benchmark for large-scale single object tracking. In *CVPR*, pages 5374–5383, 2019. 5, 6
- [26] Heng Fan, Hexin Bai, Liting Lin, Fan Yang, Peng Chu, Ge Deng, Sijia Yu, Mingzhen Huang, Juehuan Liu, Yong Xu, et al. LaSOT: A high-quality large-scale single object tracking benchmark. *IJCV*, pages 439–461, 2021. 6
- [27] William Fedus, Barret Zoph, and Noam Shazeer. Switch transformers: Scaling to trillion parameter models with simple and efficient sparsity. *JMLR*, pages 1–39, 2022. 2
- [28] Qi Feng, Vitaly Ablavsky, Qinxun Bai, Guorong Li, and Stan Sclaroff. Real-time visual object tracking with natural language description. In *WACV*, pages 700–709, 2020. 7
- [29] Qi Feng, Vitaly Ablavsky, Qinxun Bai, and Stan Sclaroff. Siamese natural language tracker: Tracking by natural language descriptions with siamese trackers. In *CVPR*, pages 5851–5860, 2021. 7

- [30] Shenyuan Gao, Chunlun Zhou, Chao Ma, Xinggang Wang, and Junsong Yuan. AiATrack: Attention in attention for transformer visual tracking. In *ECCV*, pages 146–164, 2022. 2
- [31] Goutam Yelluru Gopal and Maria A Amer. Separable self and mixed attention transformers for efficient object tracking. In *WACV*, pages 6708–6717, 2024. 2
- [32] Mingzhe Guo, Zhipeng Zhang, Heng Fan, and Liping Jing. Divert more attention to vision-language tracking. In *NeurIPS*, pages 4446–4460, 2022. 2
- [33] Kaiming He, Xiangyu Zhang, Shaoqing Ren, and Jian Sun. Deep residual learning for image recognition. In *CVPR*, pages 770–778, 2016. 2
- [34] Kaijie He, Canlong Zhang, Sheng Xie, Zhixin Li, and Zhiwen Wang. Target-aware tracking with long-term context attention. In *AAAI*, pages 773–780, 2023. 1
- [35] Geoffrey Hinton, Oriol Vinyals, and Jeff Dean. Distilling the knowledge in a neural network. *arXiv preprint arXiv:1503.02531*, 2015. 2
- [36] Lingyi Hong, Shilin Yan, Renrui Zhang, Wanyun Li, Xinyu Zhou, Pinxue Guo, Kaixun Jiang, Yiting Chen, Jinglun Li, Zhaoyu Chen, and Wenqiang Zhang. Onetracker: Unifying visual object tracking with foundation models and efficient tuning. In *CVPR*, pages 19079–19091, 2024. 1, 2, 6, 7
- [37] Xiaojun Hou, Jiazheng Xing, Yijie Qian, Yaowei Guo, Shuo Xin, Junhao Chen, Kai Tang, Mengmeng Wang, Zhengkai Jiang, Liang Liu, and Yong Liu. Sdstrack: Self-distillation symmetric adapter learning for multi-modal visual object tracking. In *CVPR*, pages 26551–26561, 2024. 1, 2, 6, 7
- [38] Lianghua Huang, Xin Zhao, and Kaiqi Huang. GOT-10k: A large high-diversity benchmark for generic object tracking in the wild. *IEEE TPAMI*, pages 1562–1577, 2019. 5, 6
- [39] Tianrui Hui, Zizheng Xun, Fengguang Peng, Junshi Huang, Xiaoming Wei, Xiaolin Wei, Jiao Dai, Jizhong Han, and Si Liu. Bridging search region interaction with template for RGB-T tracking. In *CVPR*, pages 13630–13639, 2023. 7
- [40] Eric Jang, Shixiang Gu, and Ben Poole. Categorical reparameterization with gumbel-softmax. In *ICLR*, 2017. 5
- [41] Ben Kang, Xin Chen, Dong Wang, Houwen Peng, and Huchuan Lu. Exploring lightweight hierarchical vision transformers for efficient visual tracking. In *ICCV*, pages 9612–9621, 2023. 1, 2, 6
- [42] Ben Kang, Xin Chen, Simiao Lai, Yang Liu, Yi Liu, and Dong Wang. Exploring enhanced contextual information for video-level object tracking. In *AAAI*, pages 4194–4202, 2025. 6
- [43] Ben Kang, Xin Chen, Jie Zhao, Chunjuan Bo, Dong Wang, and Huchuan Lu. Exploiting lightweight hierarchical vit and dynamic framework for efficient visual tracking. *IJCV*, pages 1–23, 2025. 6
- [44] Matej Kristan, Jiří Matas, Aleš Leonardis, Michael Felsberg, Roman Pflugfelder, Joni-Kristian Kämäräinen, Hyung Jin Chang, Martin Danelljan, Luka Čehovin, Alan Lukežič, et al. The ninth visual object tracking vot2021 challenge results. In *ICCVW*, pages 2711–2738, 2021. 6
- [45] Matej Kristan, Aleš Leonardis, Jiří Matas, Michael Felsberg, Roman Pflugfelder, Joni-Kristian Kämäräinen, Hyung Jin Chang, Martin Danelljan, Luka Čehovin Zajc, Alan Lukežič, et al. The tenth visual object tracking vot2022 challenge results. In *ECCVW*, pages 431–460, 2023. 6
- [46] Alex Krizhevsky, Ilya Sutskever, and Geoffrey E Hinton. Imagenet classification with deep convolutional neural networks. In *NeurIPS*, pages 1106–1114, 2012. 2
- [47] Hei Law and Jia Deng. CornerNet: Detecting objects as paired keypoints. In *ECCV*, pages 734–750, 2018. 5
- [48] Dmitry Lepikhin, HyoukJoong Lee, Yuanzhong Xu, Dehao Chen, Orhan Firat, Yanping Huang, Maxim Krikun, Noam Shazeer, and Zhifeng Chen. Gshard: Scaling giant models with conditional computation and automatic sharding. In *ICLR*, 2021. 2
- [49] Chenglong Li, Xinyan Liang, Yijuan Lu, Nan Zhao, and Jin Tang. RGB-T object tracking: Benchmark and baseline. *PR*, page 106977, 2019. 7
- [50] Chenglong Li, Wanlin Xue, Yaqing Jia, Zhichen Qu, Bin Luo, Jin Tang, and Dengdi Sun. LasHeR: A large-scale high-diversity benchmark for RGBT tracking. *IEEE TIP*, pages 392–404, 2021. 5, 7
- [51] Xin Li, Yuqing Huang, Zhenyu He, Yaowei Wang, Huchuan Lu, and Ming-Hsuan Yang. CiteTracker: Correlating image and text for visual tracking. In *ICCV*, pages 9974–9983, 2023. 7
- [52] Zhenyang Li, Ran Tao, Efstratios Gavves, Cees GM Snoek, and Arnold WM Smeulders. Tracking by natural language specification. In *CVPR*, pages 6495–6503, 2017. 5, 7
- [53] Liting Lin, Heng Fan, Zhipeng Zhang, Yaowei Wang, Yong Xu, and Haibin Ling. Tracking meets lora: Faster training, larger model, stronger performance. In *ECCV*, pages 300–318, 2024. 1
- [54] Tsung-Yi Lin, Michael Maire, Serge J. Belongie, Lubomir D. Bourdev, Ross B. Girshick, James Hays, Pietro Perona, Deva Ramanan, Piotr Dollár, and C. Lawrence Zitnick. Microsoft COCO: Common objects in context. In *ECCV*, pages 740–755, 2014. 5
- [55] Chang Liu, Xiao-Fan Chen, Chun-Juan Bo, and Dong Wang. Long-term visual tracking: review and experimental comparison. *Machine Intelligence Research*, pages 512–530, 2022. 2
- [56] Chang Liu, Ziqi Guan, Simiao Lai, Yang Liu, Huchuan Lu, and Dong Wang. Emtrack: Efficient multimodal object tracking. *IEEE TCSVT*, pages 2202–2214, 2024. 6, 7
- [57] Chang Liu, Yongsheng Yuan, Xin Chen, Huchuan Lu, and Dong Wang. Spatial-temporal initialization dilemma: towards realistic visual tracking. *Visual Intelligence*, page 35, 2024. 2
- [58] Ye Liu, Xiao-Yuan Jing, Jianhui Nie, Hao Gao, Jun Liu, and Guo-Ping Jiang. Context-aware three-dimensional mean-shift with occlusion handling for robust object tracking in RGB-D videos. *IEEE TMM*, pages 664–677, 2018. 2
- [59] Ze Liu, Yutong Lin, Yue Cao, Han Hu, Yixuan Wei, Zheng Zhang, Stephen Lin, and Baining Guo. Swin transformer:

- Hierarchical vision transformer using shifted windows. In *ICCV*, pages 10012–10022, 2021. 2
- [60] Ilya Loshchilov and Frank Hutter. Decoupled weight decay regularization. In *ICLR*, pages 1–9, 2018. 5
- [61] Ding Ma and Xiangqian Wu. Capsule-based object tracking with natural language specification. In *ACM MM*, pages 1948–1956, 2021. 2
- [62] Ding Ma and Xiangqian Wu. Tracking by natural language specification with long short-term context decoupling. In *ICCV*, pages 14012–14021, 2023. 7
- [63] Yinchao Ma, Yuyang Tang, Wenfei Yang, Tianzhu Zhang, Jinpeng Zhang, and Mengxue Kang. Unifying visual and vision-language tracking via contrastive learning. In *AAAI*, pages 4107–4116, 2024. 7
- [64] Christoph Mayer, Martin Danelljan, Goutam Bhat, Matthieu Paul, Danda Pani Paudel, Fisher Yu, and Luc Van Gool. Transforming model prediction for tracking. In *CVPR*, pages 8731–8740, 2022. 2
- [65] Matthias Muller, Adel Bibi, Silvio Giancola, Salman Alsubaihi, and Bernard Ghanem. TrackingNet: A large-scale dataset and benchmark for object tracking in the wild. In *ECCV*, pages 300–317, 2018. 5, 6
- [66] Hyeonseob Nam and Bohyung Han. Learning multi-domain convolutional neural networks for visual tracking. In *CVPR*, pages 4293–4302, 2016. 2
- [67] Wonpyo Park, Dongju Kim, Yan Lu, and Minsu Cho. Relational knowledge distillation. In *CVPR*, pages 3967–3976, 2019. 2
- [68] Liang Peng, Junyuan Gao, Xinran Liu, Weihong Li, Shao-hua Dong, Zhipeng Zhang, Heng Fan, and Libo Zhang. Vasttrack: Vast category visual object tracking. In *NeurIPS*, pages 130797–130818, 2024. 5
- [69] Joan Puigcerver, Carlos Riquelme Ruiz, Basil Mustafa, and Neil Houlsby. From sparse to soft mixtures of experts. In *ICLR*, 2024. 2
- [70] Yanlin Qian, Song Yan, Alan Lukežič, Matej Kristan, Joni-Kristian Kämäräinen, and Jiří Matas. Dal: A deep depth-aware long-term tracker. In *ICPR*, pages 7825–7832, 2021. 2
- [71] Alec Radford, Jong Wook Kim, Chris Hallacy, Aditya Ramesh, Gabriel Goh, Sandhini Agarwal, Girish Sastry, Amanda Askell, Pamela Mishkin, Jack Clark, et al. Learning transferable visual models from natural language supervision. In *ICML*, pages 8748–8763, 2021. 2, 3
- [72] Hamid Rezaatoughi, Nathan Tsoi, JunYoung Gwak, Amir Sadeghian, Ian D. Reid, and Silvio Savarese. Generalized intersection over union: A metric and a loss for bounding box regression. In *CVPR*, pages 658–666, 2019. 5
- [73] Carlos Riquelme, Joan Puigcerver, Basil Mustafa, Maxim Neumann, Rodolphe Jenatton, André Susano Pinto, Daniel Keysers, and Neil Houlsby. Scaling vision with sparse mixture of experts. In *NeurIPS*, pages 8583–8595, 2021. 2
- [74] Adriana Romero, Nicolas Ballas, Samira Ebrahimi Kahou, Antoine Chassang, Carlo Gatta, and Yoshua Bengio. Fittnets: Hints for thin deep nets. In *ICLR*, 2015. 2
- [75] Victor Sanh, Lysandre Debut, Julien Chaumond, and Thomas Wolf. Distilbert, a distilled version of bert: smaller, faster, cheaper and lighter. *arXiv preprint arXiv:1910.01108*, 2019. 2
- [76] Liangtao Shi, Bineng Zhong, Qihua Liang, Ning Li, Shengping Zhang, and Xianxian Li. Explicit visual prompts for visual object tracking. In *AAAI*, pages 4838–4846, 2024. 1
- [77] Jie Song, Ying Chen, Jingwen Ye, and Mingli Song. Spot-adaptive knowledge distillation. *IEEE TIP*, pages 3359–3370, 2022. 2
- [78] Zhangyong Tang, Tianyang Xu, Zhen-Hua Feng, Xuefeng Zhu, He Wang, Pengcheng Shao, Chunyang Cheng, Xiaojun Wu, Muhammad Awais, Sara Atito, et al. Revisiting RGBT tracking benchmarks from the perspective of modality validity: A new benchmark, problem, and solution. *CoRR*, 2024. 2
- [79] Yunjie Tian, Lingxi Xie, Jihao Qiu, Jianbin Jiao, Yaowei Wang, Qi Tian, and Qixiang Ye. Fast-itpn: Integrally pre-trained transformer pyramid network with token migration. *IEEE TPAMI*, pages 1–15, 2024. 5
- [80] Frederick Tung and Greg Mori. Similarity-preserving knowledge distillation. In *ICCV*, pages 1365–1374, 2019. 2
- [81] Hongyu Wang, Xiaotao Liu, Yifan Li, Meng Sun, Dian Yuan, and Jing Liu. Temporal adaptive RGBT tracking with modality prompt. In *AAAI*, pages 5436–5444, 2024. 7
- [82] Xiao Wang, Xiujun Shu, Zhipeng Zhang, Bo Jiang, Yaowei Wang, Yonghong Tian, and Feng Wu. Towards more flexible and accurate object tracking with natural language: Algorithms and benchmark. In *CVPR*, pages 13763–13773, 2021. 5, 7
- [83] Xiao Wang, Jianing Li, Lin Zhu, Zhipeng Zhang, Zhe Chen, Xin Li, Yaowei Wang, Yonghong Tian, and Feng Wu. Vi-sevent: Reliable object tracking via collaboration of frame and event flows. *IEEE TCYB*, pages 1997–2010, 2024. 5, 7
- [84] Qingmao Wei, Bi Zeng, Jianqi Liu, Li He, and Guotian Zeng. Litetrack: Layer pruning with asynchronous feature extraction for lightweight and efficient visual tracking. In *ICRA*, pages 4968–4975, 2024. 2
- [85] Xing Wei, Yifan Bai, Yongchao Zheng, Dahu Shi, and Yihong Gong. Autoregressive visual tracking. In *CVPR*, pages 9697–9706, 2023. 6
- [86] Zongwei Wu, Jilai Zheng, Xiangxuan Ren, Florin-Alexandru Vasluiianu, Chao Ma, Danda Pani Paudel, Luc Van Gool, and Radu Timofte. Single-model and any-modality for video object tracking. In *CVPR*, pages 19156–19166, 2024. 2, 6, 7
- [87] Yun Xiao, Mengmeng Yang, Chenglong Li, Lei Liu, and Jin Tang. Attribute-based progressive fusion network for RGBT tracking. In *AAAI*, pages 2831–2838, 2022. 2
- [88] Jinxia Xie, Bineng Zhong, Zhiyi Mo, Shengping Zhang, Liangtao Shi, Shuxiang Song, and Rongrong Ji. Autoregressive queries for adaptive tracking with spatio-temporal transformers. In *CVPR*, pages 19300–19309, 2024. 1
- [89] Bin Yan, Houwen Peng, Jianlong Fu, Dong Wang, and Huchuan Lu. Learning spatio-temporal transformer for visual tracking. In *ICCV*, pages 10448–10457, 2021. 6
- [90] Bin Yan, Houwen Peng, Kan Wu, Dong Wang, Jianlong Fu, and Huchuan Lu. LightTrack: Finding Lightweight Neural

- Networks for Object Tracking via One-Shot Architecture Search. In *CVPR*, pages 15180–15189, 2021. 2, 6
- [91] Song Yan, Jinyu Yang, Jani Käpylä, Feng Zheng, Aleš Leonardis, and Joni-Kristian Kämäräinen. DepthTrack: Unveiling the power of RGBD tracking. In *ICCV*, pages 10725–10733, 2021. 5, 6
- [92] Jinyu Yang, Zhe Li, Feng Zheng, Ales Leonardis, and Jingkuan Song. Prompting for multi-modal tracking. In *ACMMM*, pages 3492–3500, 2022. 7
- [93] Botao Ye, Hong Chang, Bingpeng Ma, Shiguang Shan, and Xilin Chen. Joint feature learning and relation modeling for tracking: A one-stream framework. In *ECCV*, pages 341–357, 2022. 5, 6, 7
- [94] Sergey Zagoruyko and Nikos Komodakis. Paying more attention to attention: Improving the performance of convolutional neural networks via attention transfer. In *ICLR*, 2017. 2
- [95] Pengyu Zhang, Jie Zhao, Chunjuan Bo, Dong Wang, Huchuan Lu, and Xiaoyun Yang. Jointly modeling motion and appearance cues for robust RGB-T tracking. *IEEE TIP*, pages 3335–3347, 2021. 2
- [96] Tianlu Zhang, Qiang Zhang, Kurt Debattista, and Jungong Han. Cross-modality distillation for multi-modal tracking. *IEEE TPAMI*, pages 5847–5865, 2025. 6, 7
- [97] Borui Zhao, Quan Cui, Renjie Song, Yiyu Qiu, and Jiajun Liang. Decoupled knowledge distillation. In *CVPR*, pages 11953–11962, 2022. 2
- [98] Haojie Zhao, Xiao Wang, Dong Wang, Huchuan Lu, and Xiang Ruan. Transformer vision-language tracking via proxy token guided cross-modal fusion. *PRL*, pages 10–16, 2023. 7
- [99] Jie Zhao, Jingshu Zhang, Dongdong Li, and Dong Wang. Vision-based anti-uav detection and tracking. *TITS*, pages 25323–25334, 2022. 1
- [100] Yaozong Zheng, Bineng Zhong, Qihua Liang, Zhiyi Mo, Shengping Zhang, and Xianxian Li. ODtrack: Online dense temporal token learning for visual tracking. In *AAAI*, pages 7588–7596, 2024. 1
- [101] Li Zhou, Zikun Zhou, Kaige Mao, and Zhenyu He. Joint visual grounding and tracking with natural language specification. In *CVPR*, pages 23151–23160, 2023. 7
- [102] Jiawen Zhu, Simiao Lai, Xin Chen, Dong Wang, and Huchuan Lu. Visual prompt multi-modal tracking. In *CVPR*, pages 9516–9526, 2023. 2, 6, 7
- [103] Jiawen Zhu, Huayi Tang, Xin Chen, Xinying Wang, Dong Wang, and Huchuan Lu. Two-stream beats one-stream: Asymmetric siamese network for efficient visual tracking. In *AAAI*, pages 10959–10967, 2025. 2, 6
- [104] Xue-Feng Zhu, Tianyang Xu, Zhangyong Tang, Zucheng Wu, Haodong Liu, Xiao Yang, Xiao-Jun Wu, and Josef Kittler. RGBD1K: A large-scale dataset and benchmark for RGB-D object tracking. In *AAAI*, pages 3870–3878, 2023. 6